Int. J. Heat Mass Transfer. Vol. 12, pp. 689–697. Pergamon Press 1969. Printed in Great Britain

NON-DIFFUSE INFRARED EMISSION FROM THE LUNAR SURFACE

JAMES K. HARRISON

George C. Marshall Space Flight Center, Space Sciences Laboratory, Marshall Space Flight Center, Alabama 35812

(*Received* 26 *June* 1968 *and in revised form* 4 *November* 1968)

Abstract—This paper presents the results of calculations of the thermal radiation from the lunar surface incident onto a flat surface of unit area located a small distance above the Moon. The orientation and height of the flat surface vary. The thermal radiation from the Moon's surface is assumed to be non-diffuse.

The calculations show that the thermal energy flux incident onto the flat surface can differ significantly for a lunar surface that emits radiation in a non-diffuse manner when compared to a lunar surface that emits in a diffuse manner.

NOMENCLATURE

I_0,	i.r. radiance [W/m^2-sr];
I,	i.r. energy [W/m^2-sr];
a_1, a_2, a_3, a_4,	empirically determined constants;
$i, \epsilon, \phi_i, \phi_\epsilon, \alpha$,	angles; see Fig. 3;
r,	distance from dA_1 to dA_2 [m];
E,	energy flux from A_1 to dA_2 [W/m^2];
A_1,	lunar surface area; assumed circular [m^2];
dA_2,	unit element [m^2];
$\bar{h}$,	height of dA_2 above lunar surface [m];
R,	radius of A_1 [m];
$\phi^*, \phi^{**}, \phi^{***}$,	limits of integration;
T_B,	lunar surface brightness temperature [°K];
σ,	Stefan–Boltzmann constant [$5{\cdot}673 \times 10^{-8}$ W/m^2-°K^4];
θ,	angle; see Fig. 3;
γ, ϕ_2,	elevation and azimuthal orientation angle of dA_2 (see Fig. 5);
ω,	sun elevation angle (see Fig. 5).

INTRODUCTION

THIS research program in directional i.r. radiation is an attempt to partially fulfill the goal of explaining and defining the lunar thermal environment. One part of the directional radiation program is to develop a theoretical model with which one can accurately reproduce the existing experimental data and that is consistent with current knowledge of the physical structure of the Moon's surface. Such a model should reveal important information about the physical features of the surface. Another part of the program is to present information about the directional aspects in a form useful to those solving problems in thermal experiments and thermal studies of the Moon's surface. This report represents an effort to partially fulfill this last part. Calculations have been performed incorporating these directional effects; the results are graphically presented as i.r. energy leaving the lunar surface and striking a unit area a small distance away.

To support the in-house work, a number of contracts have been sponsored with outside research organizations. In 1965 a contract with Brown Engineering Co. led to an arrangement whereby one member of the Brown research staff spent 6 months at the Boeing Scientific Research Laboratories working closely with Saari and Shorthill. These two investigators have obtained an extensive amount of data over the past 5 years on the i.r. emission from the Moon [1]. Their measurements have been in the 10 to 12 μ region of the spectrum. The purpose of the work between Brown and Boeing was to obtain from existing data a new set of measurements relating to the directional characteristics of lunar i.r. emission. The effort consisted mainly of a reduction of many data points from 19 separate phases. The data were then presented graphically [2] in the form of brightness temperatures† for various lunar locations and phases. A typical graph is shown in Fig. 1.

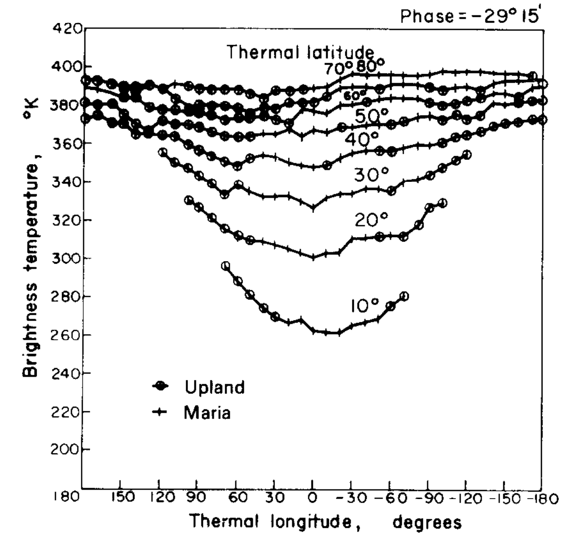

FIG. 1. Lunar brightness temperature for a single phase and various lunar locations.
(a) Brightness temperature v. thermal longitude at phase −29°15′.
(b) Thermal coordinate grid for phase angle −29°15′.

Using the experimental results from the foregoing work and working under the sponsorship of the Space Sciences Laboratory, Ashby and Burkhard have developed an expression for predicting the i.r. emission that takes into account the directional behavior of the radiation [3]; comparisons with experimental data show it to be reasonably accurate.‡

When the work was first begun, the only experimental i.r. data that had been examined (to the author's knowledge) for any directional characteristics were those of Pettit and Nicholson [4] and Sinton [5], and these data showed only a slight deviation from a Lambertian surface emission. It has been known for some time that sunlight is reflected by the Moon's surface in a strongly directional manner. Although this is in a different part of the spectrum from the infrared, it did help to stimulate an initial interest in taking a closer look at the directional aspects of the i.r. emission. The Pettit, Nicholson, and Sinton data and the photometric data were the basis for the speculation that the emission might be directional to a significant degree and deserved further investigation.

Measurements from Surveyor I in 1966 indicated that a directional emission did exist and that it was more pronounced than previously observed. The explanation of the temperature values recorded on the faces of the two instrument compartments of Surveyors I and III [6, 7] has involved these directional effects although not explaining fully the behavior of all of the temperature measurements. Investigations by Saari and Shorthill [8] subsequent to Surveyor I of their Earth-based measurements have also affirmed the presence of the directional effects.

Some of the Saari and Shorthill data showing the directional aspects are presented in Fig. 2. Measured results from Earth-based telescopes are compared with calculated results using the previously mentioned Ashby expression. For each elevation angle of the Sun, the brightness temperature is shown (for a diffuse surface the brightness temperature is a single point and is shown as an open circle). By comparing the diffuse value with the non-diffuse points, the degree of directionality can be ascertained. Notice that the radiation exhibits the greatest non-diffuseness, i.e. directionality for small Sun elevation angles. Another point to notice is that the largest temperature values occur, for each Sun elevation angle, when the surface is viewed from the Sun direction: that is when an observer views the surface with the Sun behind him.

† Brightness temperature is the temperature of a black-body radiating the same amount of energy per unit area at the wavelengths under consideration (here 10 to 12 μ) as the observed body, i.e. the Moon.

‡ Further work is needed in this area to relate this empirically determined expression to the physical characteristics of the lunar surface.

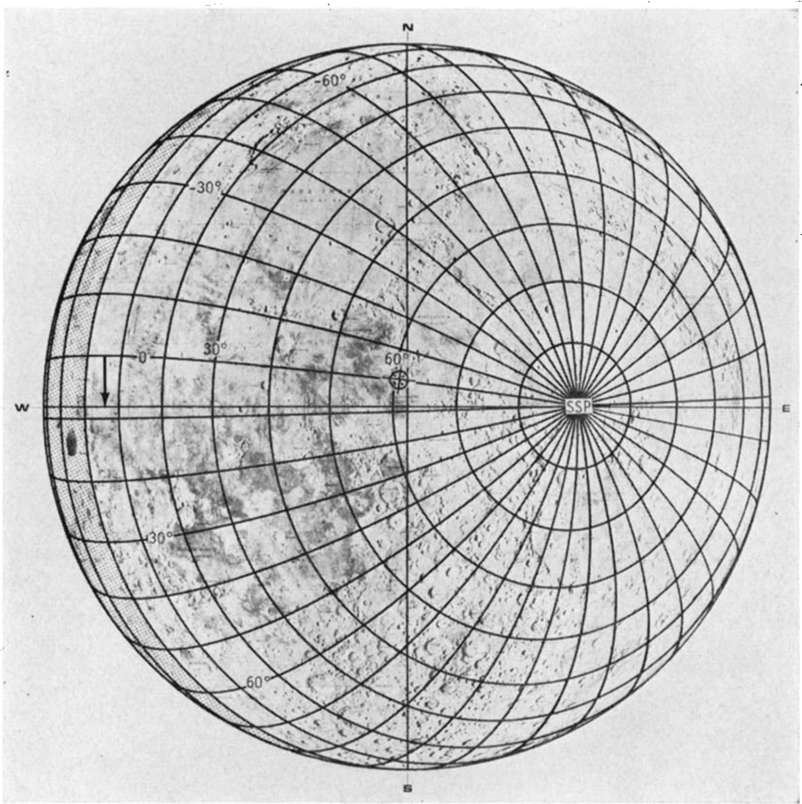

(b). Thermal coordinate grid for phase angle −29° 15′.

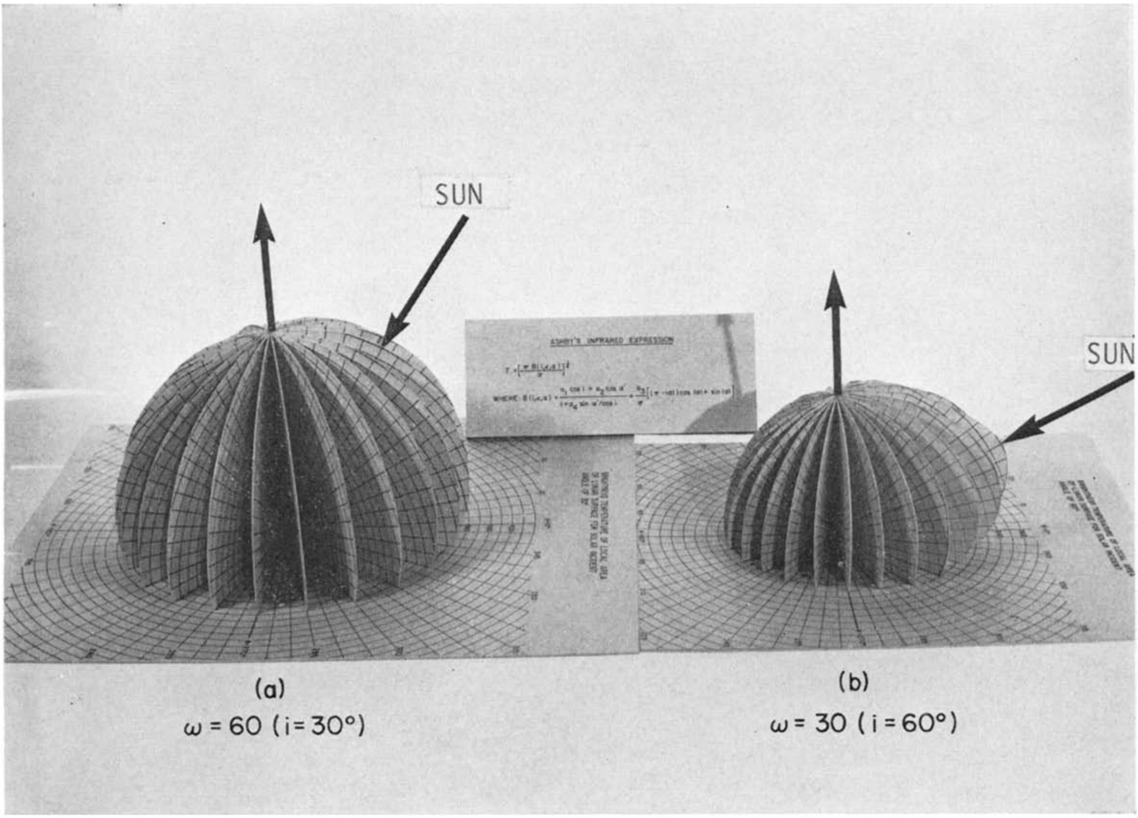

(a) $\omega = 60°$ $(i = 30°)$
(b) $\omega = 30°$ $(i = 60°)$

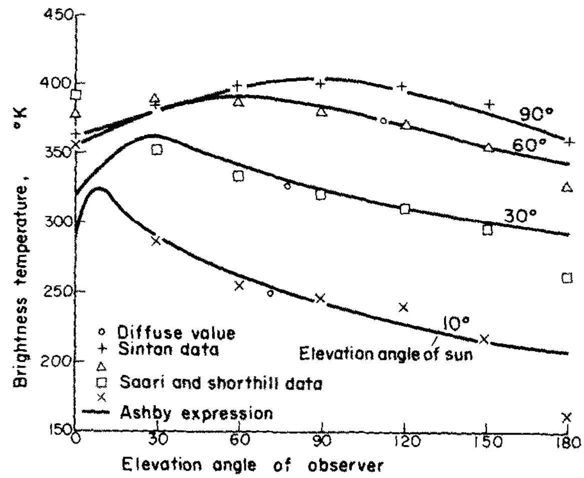

FIG. 2. Lunar brightness temperatures as a function of the angle of observation for several elevation angles of the Sun.

This means that a greater part of the i.r. radiation is emitted toward the source, i.e. the Sun, than in any other direction. Such behavior may be referred to as back-emitted, a term analogous to backscatter for the reflected sunlight from the Moon that is reflected or scattered more toward the source than in any other direction.

Gross surface roughness has been suggested as the reason for the back-emitted directional radiation. This thought was put forth by Pettit and Nicholson to explain their measurements of non-diffuse radiation and still appears to be the most satisfactory explanation. The surface, if assumed to consist of peaks and valleys (or of numerous craters and rocks), will receive sunlight mainly on the side facing the Sun. The other side will be in the shadow and will, therefore, be at a much lower temperature. This condition will exist to the greatest degree when the Sun is near the horizon, and to the least degree (or not at all) when the Sun is straight overhead.

The Earth-based measurements were made with telescopes that have resolutions of the order of 8–10 sec of arc. At the lunar distance, this means that the measurements average the radiation (at the Moon's center) over a circular region of approximately 14 to 18 km in diameter. Whether the measurements would reveal this same directional characteristic over a much smaller region, say on the order of a few meters, is an unanswered question. The surface would probably be more diffuse. The reason given earlier—gross surface roughness—would not suffice to explain any directional behavior observed on this scale.

THERMAL EMISSION PER UNIT SOLID ANGLE

The emission of i.r. energy from a local area on the Moon in a given direction can be computed from Lambert's equation, $I(\epsilon) = I_0 \cos \epsilon$, if the emission is assumed to be diffuse. However, if the emission is non-diffuse as recent data indicate [7], the i.r. emission from a local area on the Moon in a given direction can be more accurately determined from the following expression, which was developed under a NASA contract [3].

$$I_0(i, \epsilon, \alpha) = \frac{a_1 \cos i + a_2 \cos \alpha'}{1 + a_4(\sin \alpha'/\cos i)} + \frac{a_3}{\pi}[(\pi - |\alpha|)\cos|\alpha| + \sin|\alpha|] \qquad (1)$$

where:

$$\alpha' = \frac{\pi}{2}\sqrt{\left(\frac{i^2 + \epsilon^2 - 2i\epsilon\cos(\phi_i - \phi_\epsilon)}{(\pi^2/4) + (4i^2\epsilon^2/\pi^2) - 2i\epsilon\cos(\phi_i - \phi_\epsilon)}\right)}$$

$I_0(i, \epsilon, \alpha)$ = i.r. radiance in W/m^2-sr
$a_1 = 335$
$a_2 = 97{\cdot}6$
$a_3 = 51{\cdot}6$
$a_4 = 0{\cdot}121$
(All of the a's are empirically determined using the Saari and Shorthill data of [1] and [2]. All except a_4, which is dimensionless, have units of W/m^2-sr.) $i, \varepsilon, \phi_i, \phi_\epsilon, \alpha$ = Angles defined in Fig. 3.

This expression holds true only for a sunlit surface; therefore, it is not useful during the lunar night or for lunar areas that are completely in shadow. From equation (1) the i.r. energy is

$$I(i, \epsilon, \alpha) = I_0(i, \epsilon, \alpha)\cos \epsilon. \qquad (2)$$

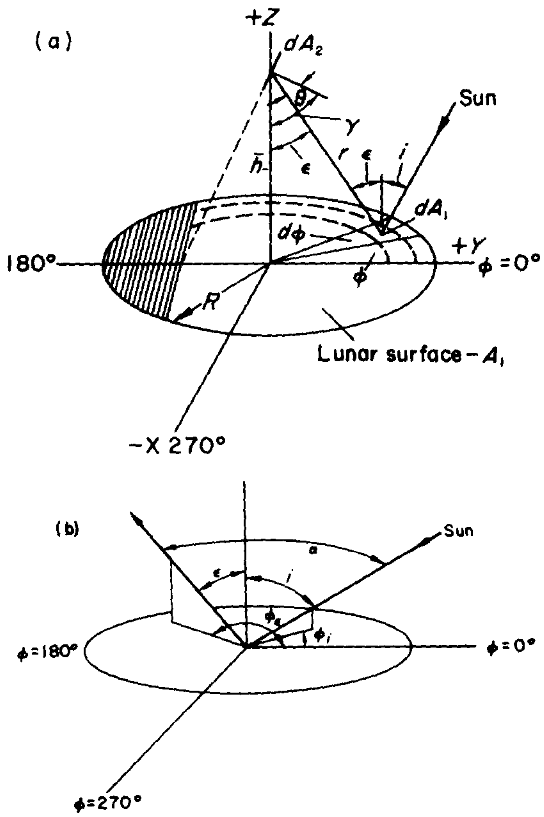

FIG. 3. Angles involved in discussion and calculations (a) Angles involved in integration of equation (10). (b) Angles used in equation (1).

The brightness temperature of a local lunar area when observed from different directions and for different Sun elevation angles can be obtained from equation (1) as follows:

$$T_B = \left[\frac{\pi I_0(i, \epsilon, \alpha)}{\sigma}\right]^{\frac{1}{4}} \qquad (3)$$

where σ = Stefan–Boltzmann constant ($5{\cdot}673 \times 10^{-8}$ W/m^2-°K^4). The brightness temperature as obtained from equation (3) for two sun elevation angles are shown in Fig. 4.

TOTAL THERMAL EMISSION

If the i.r. emission in the direction of dA_2 from many local areas, such as dA_1 (Fig. 3), is summed over a local lunar surface area A_1, the energy incident onto dA_2 can be determined. The energy from dA_1 to dA_2 is found by using equation (4) below. The angles ϵ and θ are required to compensate for the skewness of the surfaces with respect to each other, while the term r^2 represents the attenuation of the energy in accordance with the inverse square law.

$$\mathrm{d}E = \frac{I_0(i, \epsilon, \alpha) \cos \epsilon \cos \theta}{r^2} \mathrm{d}A_1 \, \mathrm{d}A_2 \qquad (4)$$

where $\mathrm{d}E$ is the energy flux from $\mathrm{d}A_1$ to $\mathrm{d}A_2$ in W.

The lunar area A_1 is taken as flat and circular with a radius R. Summing over A_1 and assuming $\mathrm{d}A_2$ to be unity gives

$$E = \int_{A_1} \frac{I_0(i, \epsilon, \alpha) \cos \epsilon \cos \theta}{r^2} \mathrm{d}A_1 \qquad (5)$$

where E is the energy flux from A_1 to $\mathrm{d}A_2$ in W/m^2.

Formulating r and $\mathrm{d}A_1$ in terms of the fundamental angles gives

$$\mathrm{d}A_1 = \bar{h}^2 \tan \epsilon \sec^2 \epsilon \, \mathrm{d}\phi \, \mathrm{d}\epsilon \qquad (6)$$

$$r = \bar{h} \sec \epsilon. \qquad (7)$$

Substituting equations (6) and (7) back into equation (5) gives

$$E = \int_0^{\tan^{-1} R/\bar{h}} \int_0^{2\pi} I_0(i, \epsilon, \alpha) \cos \theta \sin \epsilon \, \mathrm{d}\phi \, \mathrm{d}\epsilon. \qquad (8)$$

The angle θ can be obtained for any orientation of $\mathrm{d}A_2$ and in terms of ϵ, γ, and ϕ by

$$\theta = \cos^{-1} [\cos \epsilon \cos \gamma - \sin \epsilon \cos (180 - \phi) \sin \gamma], \ \theta < \pi/2 \qquad (9)$$

$$\theta = \pi/2, \ \theta \geqslant \pi/2.$$

Because of the limits of integration, the integration over ϕ is done in four parts—one part for each quadrant of A_1. Finally,

$$E = \int_0^{\tan^{-1} R/\bar{h}} \int_0^{\phi^{**}} I_0(i, \epsilon, \alpha) \cos \theta \sin \epsilon \, \mathrm{d}\phi \, \mathrm{d}\epsilon$$
$$+ \int_0^{\tan^{-1} R/\bar{h}} \int_{\pi/2}^{\pi - \phi^{*}} I_0(i, \epsilon, \alpha) \cos \theta \sin \epsilon \, \mathrm{d}\phi \, \mathrm{d}\epsilon$$
$$+ \int_0^{\tan^{-1} R/\bar{h}} \int_{\pi + \phi^{*}}^{3\pi/2} I_0(i, \epsilon, \alpha) \cos \theta \sin \epsilon \, \mathrm{d}\phi \, \mathrm{d}\epsilon$$

$$+\int_{0}^{\tan^{-1}R/\bar{h}}\int_{3\pi/2+\phi^{***}}^{2\pi} I_0(i,\epsilon,\alpha)\cos\theta\sin\epsilon\, d\phi\, d\epsilon. \quad (10)$$

The values for ϕ^*, ϕ^{**}, and ϕ^{***} depend on the orientation of dA_2. The values and corresponding orientations are as follows:

$$\begin{aligned}
\phi^* &= 0 &&; \gamma < \pi/2, 0 < \epsilon \leqslant |\gamma - 90| \\
\phi^* &= \cos^{-1}\left(\frac{\tan|\gamma - 90|}{\tan\epsilon}\right) &&; \gamma < \pi/2, |\gamma - 90| < \epsilon \leqslant \tan^{-1} R/\bar{h} \\
\phi^* &= \pi/2 &&; \gamma \geqslant \pi/2 \\
\phi^{**} &= \pi/2 &&; \gamma \leqslant \pi/2 \\
\phi^{**} &= \cos^{-1}\left(\frac{\tan|\gamma - 90|}{\tan\epsilon}\right) &&; \gamma > \pi/2, |\gamma - 90| < \epsilon \\
\phi^{**} &= 0 &&; \gamma > \pi/2, |\gamma - 90| \geqslant \epsilon \\
\phi^{***} &= 0 &&; \gamma \leqslant \pi/2 \\
\phi^{***} &= \sin^{-1}\left(\frac{\tan|\gamma - 90|}{\tan\epsilon}\right) &&; \gamma > \pi/2, |\gamma - 90| \leqslant \epsilon \leqslant \tan^{-1} R/\bar{h} \\
\phi^{***} &= \pi/2 &&; \gamma > \pi/2.
\end{aligned}$$

RESULTS OF COMPUTATIONS

Equation (10) has been integrated numerically. Figure 3 provides an explanation of the angles involved in the integration, and Fig. 5 is helpful in understanding the results. Figure 6 presents the results of the computations using equation (10). Shown on the figure is the i.r. energy flux from an area A_1 of the lunar surface (assumed to have an i.r. emittance of unity) incident onto one side only of the element A_2 for different Sun elevations. Each curve represents a different tilt angle γ for A_2 and the entire figure represents a single value for the ratio of the size of the lunar surface to the height of A_2 above the lunar surface, $R/\bar{h}$, and a single azimuthal orientation, ϕ_2, of the element. When ϕ_2 is 180°, the element faces west.

It is instructive to delineate as plainly as possible the directional aspects. One way of doing this is by comparing a diffuse and non-diffuse case for one orientation of the element, as is done in Fig. 7. As in the previous figure, energy is plotted against Sun position. A clearer way of showing the directional characteristics is by normalizing the energy values (such as given in Fig. 6) about the maximum value (the curve for $\gamma = 0$). This has been done for three azimuthal orientations, ϕ_2, of the element (additional azimuthal orientations are given in [9]. This normalized result or view factor† is more useful for performing thermal radiation calculations. Figures 8 through 10 present the view

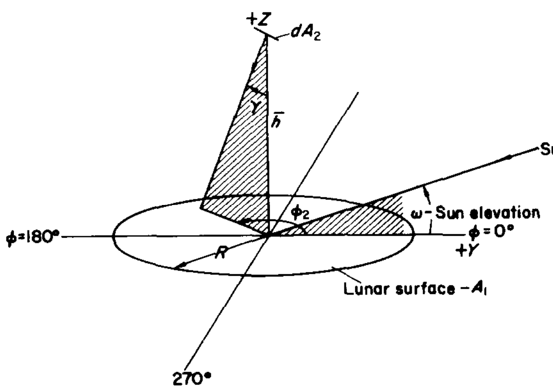

FIG. 5. Angles used in calculations of final results.

† This view factor is the one commonly used in radiation exchange calculations.

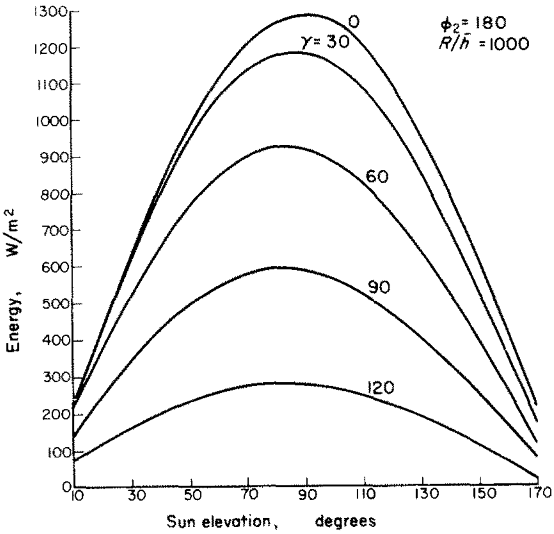

FIG. 6. Energy incident onto one side of dA_2 vs. Sun elevation angle for various orientations of dA_2 (element points west, $\phi_2 = 180°$).

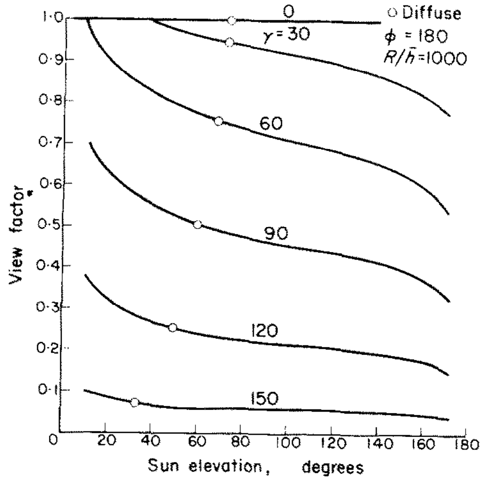

FIG. 8. View factor between lunar surface and dA_2 vs. Sun elevation angle for various orientations of dA_2 (element points west, $\phi_2 = 180°$).

factor. Figure 8 is typical of the other figures and will be used to point out some of the significant points. In Fig. 8 the element points west, i.e. $\phi_2 = 180°$. As the Sun moves from the sunrise to sunset position, the directional aspects of the radiation can be plainly seen on comparison with the diffuse value, which is shown as a single point (although it could be shown as a horizontal line through this point). Notice particularly the general shape of the curves, how the energy striking the element is greatest near sunrise, i.e. when the Sun elevation angle is small and decreases as the sun moves from this position

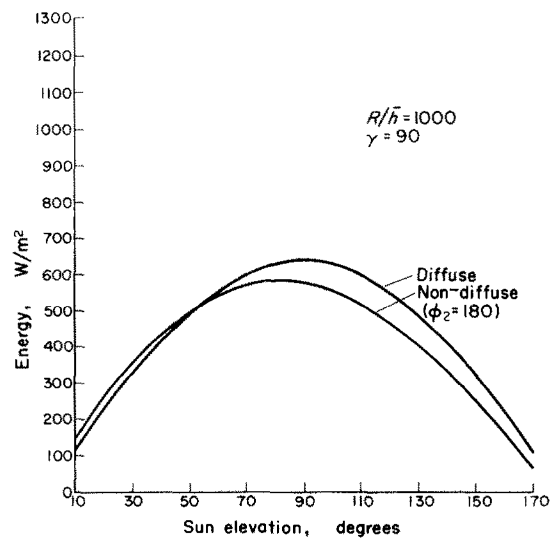

FIG. 7. Comparison of energy incident onto dA_2 for diffuse and non-diffuse cases.

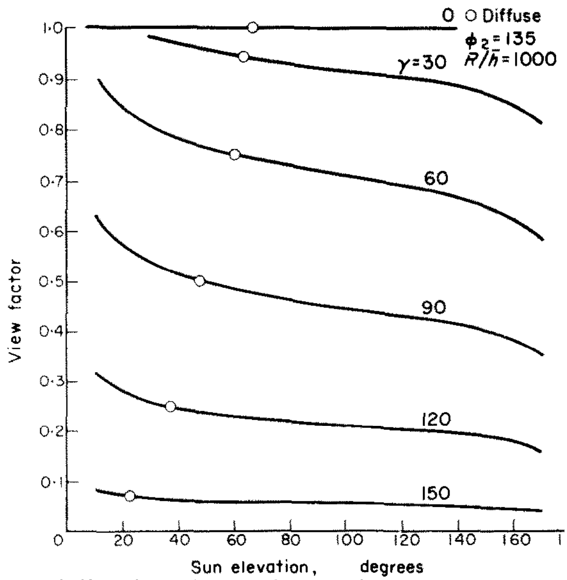

FIG. 9. View factor between lunar surface and dA_2 vs. Sun elevation angle for various orientations of dA_2 (element points northwest, $\phi_2 = 135°$).

through lunar noon, finally having the smallest view factor when the Sun is near sunset and facing the element. For an element facing east ($\phi_2 = 0°$), the shape of the curve is exactly reversed, i.e. the smallest view factor occurs at sunrise and the greatest occurs at sunset. The other figures are for elements facing in other directions. Notice the element facing north ($\phi_2 = 90°$), Fig. 10. The curves are almost flat,

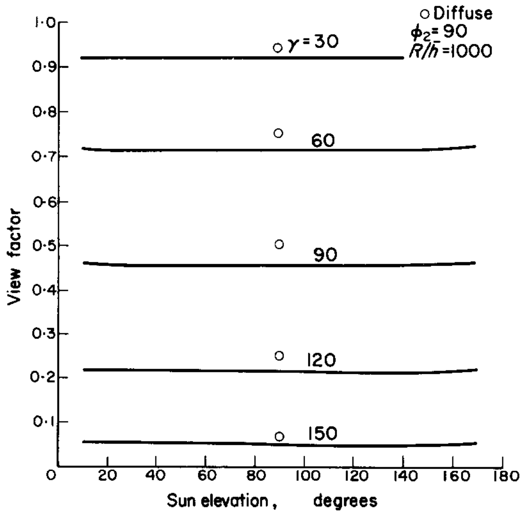

FIG. 10. View factor between lunar surface and dA_2 vs. Sun elevation angle for various orientations of dA_2 (element points north, $\phi_2 = 90°$).

meaning that almost no changes in the surface radiation occur for changing Sun angle when the lunar surface is observed from such a direction. This is somewhat evident from Fig. 4 where the shape of the model indicates the distribution of the energy. Notice that the radiation is asymmetrically in the plane containing the surface normal and the east-west axis (the plane containing the Sun vector) and symmetrical in the plane containing the surface normal and the north-south axis.

The curves shown in Figs. 8 through 10 are for an element confined to one quadrant of the azimuthal plane, i.e. $\phi_2 = 90°–180°$. For elements facing directions other than this, symmetrical considerations depicted in Figure 4 can be used to get the view factor from the values shown here. For example, the view factor values are the same for $\phi_2 = 225°$ as for $\phi_2 = 135°$. Figure 4 aids in understanding why this is so since the figure shows that the brightness temperature or energy in these two directions is the same. For $\phi_2 = 45°$, the values are the same as for $\phi_2 = 135°$, but the abscissa on the graph must be reversed, i.e. the scale should begin with 180° and end with 0°. When this is done, the view factor values that were at 30° Sun elevation (for example) will appear instead at 150° Sun elevation. This reversing scheme must always be used when the element faces between $\phi_2 = 0°–90°$ or 270°–360°.

The curves clearly show the effects of the back-emitted radiation since the largest view factor occurs when the element faces away from the Sun.

This variation of energy with element position can be shown in another way by having the element rotate about an axis vertical to the Moon's surface (i.e. rotation in the azimuthal plane) while the Sun's position is fixed. This is shown in Fig. 11. The element itself is vertical to the surface ($\gamma = 90°$) and the diffuse values are again shown as a single point. Notice that the radiation shows no change where the sun is straight overhead ($\omega = 90°$). This is because the

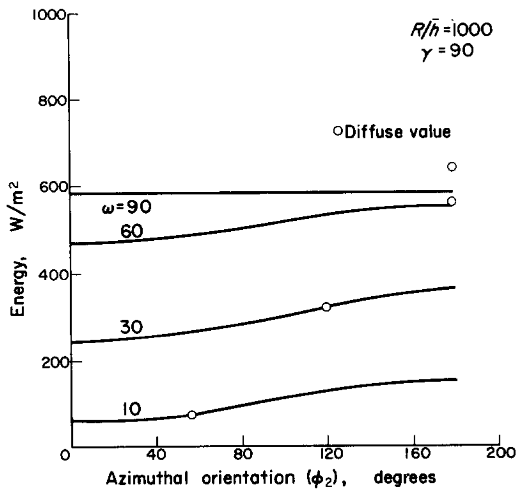

FIG. 11. Energy incident onto dA_2 while rotating dA_2 about the Z axis for various Sun elevations (ω).

radiation is symmetrical with respect to the azimuthal plane. This trend toward symmetry in the azimuthal plane as the Sun approaches lunar noon can be observed in Figs. 2 and 4. I.r. measurements of the full Moon, such as those of Pettit and Nicholson, are for this condition; and directional aspects when viewed from Earth are at a minimum.

FINAL REMARKS

One method for taking the directional aspects of the lunar surface i.r. radiation into account in numerical calculations has been shown. The results presented here have shown that calculations based on diffuse radiation may be as much as 80 W/m^2 (16 per cent of total) at variance with calculations based on non-diffuse radiation (Fig. 7). Orientation of the surface receiving the radiation and Sun position are also important. For a Sun elevation angle of 30°, the radiation striking a surface which is oriented vertically to the lunar surface may vary as much as 120 W/m^2 (33 per cent of total) as the surface is rotated 180° about a vertical axis (Fig. 11).

ACKNOWLEDGEMENTS

Wayne Griffith, Computer Sciences Corporation, did the scientific programming for this problem. Jimmy R. Watkins and Tommy C. Bannister, Space Sciences Laboratory, provided mathematical assistance.

REFERENCES

1. J. M. Saari and R. W. Shorthill, *Isothermal and Isophotic Atlas of the Moon*. NASA CR-855, September 1967.
2. C. G. Montgomery, J. M. Saari, R. W. Shorthill and N. F. Six Jr., Directional characteristics of lunar thermal emission, Brown Engineering Company, Inc., Technical Note No. R-213; Also published as Boeing Document No. D1-83-0568, November 1966.
3. N. Ashby and D. G. Burkhard, Study of radiative aspects of lunar materials, NASA CR-61481 (1967).
4. E. Pettit and S. B. Nicholson, Lunar radiation and temperatures, *Astrophys. J.* **71**, 102 (1930).
5. W. M. Sinton, Temperatures on the lunar surface, in *Physics and Astronomy of the Moon* (Edited by Z. Kopal), p. 411, Academic Press, New York (1962).
6. J. W. Lucas *et al.*, *Lunar Surface Thermal Characteristics*. Chap. IV. Surveyor I Mission Report, Part II, Scientific Data and Results. Technical Report No. 32-1023, Jet Propulsion Laboratory, California Institute of Technology, Pasadena, Calif. (1966). Also published in *J. geophys. Res.* **72**, 779–789 (1967).
7. J. W. Lucas *et al.*, *Lunar Surface Temperatures and Thermal Characteristics*, Surveyor III Mission Report, Part II: Scientific Results. Technical Report 32-1177, Jet Propulsion Laboratory California Institute of Technology, Pasadena, Calif., (1967).
8. J. M. Saari and R. W. Shorthill, Review of lunar infrared observations, *Physics of the moon*, (edited by S. F. Singer), Vol. 13, AAS Science and Technology Series (1967).
9. J. K. Harrison, Calculations of non-diffuse infrared radiation from the lunar surface incident onto a unit element above the surface, NASA TM X-1567 (1968).

Résumé—Cet article présente les résultats des calculs du rayonnement thermique à partir de la surface lunaire tombant sur une surface plane d'aire unité placée à une petite distance au-dessus de la lune. L'orientation et la hauteur de la surface plane varient. Le rayonnement thermique venant de la surface de la lune est supposé être non-diffus.

Les calcus montrent que le flux d'énergie thermique tombant sur la surface plane peut différer sensiblement pour une surface lunaire qui émet un rayonnement d'une façon non-diffuse lorsqu'on le compare à une surface lunaire qui émet d'une façon diffuse.

Zusammenfassung—Es werden Ergebnisse angegeben zur Berechnung der Wärmestrahlung, die von der Mondoberfläche auf eine ebene Einheitsfläche in geringer Entfernung über dem Mond fällt; Richtung und Höhe der Fläche werden variiert. Es wird angenommen, dass die von der Mondoberfläche ausgehende Wärmestrahlung nicht diffus ist.

Die Berechnungen zeigen, dass sich für die, auf die betrachtete Fläche fallende Strahlungsenergie beträchtliche Unterschiede ergeben zwischen diffus und nicht-diffus emittierender Mondoberfläche.

Аннотация—В статье представлены результаты расчётов термического излучения с лунной поверхности на плоскую поверхность единичной площади, расположенную на небольшом расстоянии над луной. Положение и высота плоской поверхности изменялись. Предполагалось, что термическое излучение с поверхности луны является недиффузионным. Расчёты показывают, что поток тепловой энергии, падающий на плоскую поверхность, может значительно отличаться для лунной поверхности с недиффузионным излучением от лунной поверхности с диффузионным излучением.